Ocean Sci. Discuss., 11, 1191–1212, 2014
www.ocean-sci-discuss.net/11/1191/2014/
doi:10.5194/osd-11-1191-2014

Ocean Science
Discussions
Open Access

The shallow meridional overturning circulation of the South China Sea

N. Zhang, J. Lan, and F. Cui

Physical Oceanography Laboratory, and College of Physical and Environmental Oceanography, Ocean University of China, Qing dao, China

Received: 6 March 2014 – Accepted: 4 April 2014 – Published: 30 April 2014

Correspondence to: J. Lan (lanjian@ouc.edu.cn)

Published by Copernicus Publications on behalf of the European Geosciences Union.

Abstract

In this paper, the structure and formation mechanism of the annual-mean shallow meridional overturning circulation of the South China Sea (SCS) are investigated. A distinct clockwise overturning circulation is present above 400 m in the SCS on the climatological annual mean scale. The shallow meridional overturning circulation consists of downwelling in the northern SCS, a southward subsurface branch supplying upwelling in the southern SCS and a northward return flow of surface water. The formation mechanism is explored by studying causes of the branches constituting the meridional overturning circulation. The surface branch is driven by the annual mean zonal component of the wind stress which is predominantly westward. Another effect of the wind is Ekman pumping related subduction in the north hence the main source of downwelling there. The mixed layer depth reaches its maximum in winter and shoals in spring, which causes the thermocline to outcrop and ventilate. Part of the water mass from the bottom of the mixed layer subducts into the thermocline and flows southward along the isopycnals. The upwelling region is mainly along the Vietnam coast and in the open-ocean off it. In summer, the alongshore component of wind stress off Vietnam can cause coastal upwelling and the increase of alongshore wind off the coast can also cause great upwelling in the open-ocean off the Vietnam coast.

1 Introduction

The South China Sea (SCS) is the largest marginal sea in Southeast Asia with an average depth of over 2000 m. It is located in the East Asian Monsoon area and has complicated climatic conditions. Its circulation and thermal structure are significantly influenced by the monsoon (Su, 2005).

The meridional thermohaline process accompanying the SCS upper layer overturning circulation has a great impact on the heat budget and air–sea interactions of the SCS and the adjoining oceans. Wang (2004) first simulated the SCS upper layer meridional overturning circulation with idealized bottom topography using the Geophysical Fluid Dynamics Laboratory (GFDL) general circulation model. He found that a shallow unenclosed meridional overturning circulation existed above 300 m in the SCS and that water exchange through Luzon Strait had a great impact on it. Liu (2008) showed that the seasonal variability of the intrusion of North Pacific Tropical Water (NPTW) and North Pacific Intermediate Water (NPIW) to the SCS was highly related to the seasonal variability of the SCS meridional overturning. Although some investigations have been carried out on the variability of the meridional overturning circulation, little work has been done on the study of its dynamics.

In this paper, we focus on the study of the shallow meridional overturning circulation in the SCS on the climatological annual mean scale and investigate the dynamics of its formation. This paper is organized as follows. Section 2 gives a brief description of the Simple Ocean Data Assimilation (SODA) and Ocean general circulation models for the Earth Simulator (OFES) data as well as the method to calculate the overturning circulation stream function. Section 3 describes the annual mean structure of the meridional overturning circulation. The probable dynamic mechanism of its formation is discussed in Sect. 4. Section 5 compares the shallow meridional overturning circulation in the SCS and the cross-equatorial cell in the Indian Ocean to see their similarities and differences. The results are finally summarized in Sect. 6.

2 Data and method

The SODA data used in this paper is version 2.1.6 monthly meridional velocity data (v) ranging from January 1959 to December 2008. SODA uses an ocean model based on Geophysical Fluid Dynamics Laboratory (GFDL) Modular Ocean Model 2 code (MOM2) (Carton, 2000). The horizontal spatial resolution is $0.5^\circ \times 0.5^\circ$. There are 40 levels in the vertical direction from 5.01 m to 5375 m with a finer resolution in the upper ocean. In this study we focus on the domain extending from 99° E to 121° E and 0° N to 23° N.

OFES is based on the modular ocean model (MOM3). It is run for 50 years using monthly mean wind stress and surface heat flux from National Centers for Environment Prediction and the National Center for Atmospheric Research (NCEP/NCAR), and monthly temperature and salinity fields from the World Ocean Atlas (WOA98) (Masumoto et al., 2004; Sasaki et al., 2004). The output is monthly means for the last six years (years 45–50) of a climatologically forced integration.

The meridional overturning stream function is used to study the meridional overturning circulation. The stream function is calculated from meridional velocity $v(x,y,z,t)$ as (Cabanes et al., 2008),

$$\psi(y,z,t) = \int_{-z}^{0} \int_{x_{\mathrm{east}}(y,z)}^{x_{\mathrm{west}}(y,z)} v(x,y,z,t)\mathrm{d}x\mathrm{d}z. \tag{1}$$

Here x is in zonal direction, and z is in vertical direction.

3 Structure of annual-mean SCS meridional overturning circulation

The shallow clockwise meridional overturning circulation is present between 8° N and 19° N above 400 m as revealed in plots of zonally averaged, meridional stream functions from SODA (Fig. 1a). The stream function value at a latitude and a depth denotes the total volume transported across this zonal section above this depth. Along a contour, the higher value is always at the right-hand side. Associated with the meridional overturning circulation, there is southward subsurface flow (between 50 m and 400 m) and compensating northward surface flow (above 50 m), downwelling at about 19° N and upwelling between 8–12° N, with strength of about 1 Sv. It can be seen from Fig. 1a that the peripheral part of the meridional overturning circulation, the zero contour of the stream function for example, is unenclosed at 19° N. The characteristic of being unenclosed shows that part of the subsurface cold water is not formed locally but

OSD
11, 1191–1212, 2014

transported into the SCS via Luzon Strait from the open Pacific (Wang et al., 2004). The OFES data are used here for validation, and it does show a weaker meridional overturning structure limited to a shallower depth (Fig. 1b) compared with that obtained from the SODA data.

SODA data have been widely used in the study of the SCS and validated as able to give reliable results (Wang et al., 2006; Yang et al., 2012; Song et al., 2014). It was also used in the study of the shallow meridional overturning circulation in the Indian Ocean to confirm the existence of the equatorial roll and to calculate coastal upwelling (Shott et al., 2002). Out of these considerations, we believe that SODA data are reliable in the study of the shallow meridional overturning circulation in the SCS and it will be used in the following sections.

4 Formation mechanism of the meridional overturning circulation

From what was discussed above, we know that the shallow meridional overturning circulation consists of downwelling in the northern SCS, southward subsurface branch supplying the upwelling in about 8–12° N and a return flow of surface water. In this section, we investigate the driving force of its respective branches.

4.1 Monsoon and Ekman transports

The SCS is located in the East Asian Monsoon area. The stronger northeast monsoon first appears in the northern SCS in September and then extends over the entire basin from October to February. The weaker southwest monsoon prevails during the period from mid-May to August (Shaw et al., 1994; Qu et al., 2000). The wind fields for January, April, July and October, respectively, from the NCEP monthly-mean climatology, illustrate the drastic changes of the monsoon (Fig. 2).

In the annual-mean wind stress distribution, the winter monsoon pattern dominates over the SCS basin (Fig. 3). The westward wind stress τ^x at most latitudes drives

OSD
11, 1191–1212, 2014

Shallow meridional overturning circulation of the South China Sea

N. Zhang et al.

northward Ekman transport in the surface (Fig. 4). The annual-mean Ekman transport across 18° N is about 0.91 Sv. This value is corresponding to the strength of the shallow meridional overturning circulation, which is about 1 Sv (Fig. 1). This confirms that the surface northward flow is mainly driven by the westward zonal wind component of the annual mean wind stress.

4.2 Subduction in the northern SCS

4.2.1 Ventilated thermocline in the northern SCS

In this section, the driving mechanism of the downwelling branch of the shallow meridional overturning circulation in the northern SCS is studied.

Iselin (1939) proposed the first conceptual model of water mass formation. According to his model, Ekman pumping in late winter forces water to cross the base of the Ekman layer and flow along isopycnals thereafter. Later studies also pointed out the importance of lateral induction of fluid across the sloping base of the mixed layer (Woods, 1985). The Ekman pumping and lateral induction rates composed the subduction rate (Marshall et al., 1993), which plays an important role in the vertical movement of water mass. As there is great negative wind stress curl in the northern SCS (Fig. 3), we speculate that subduction is the cause of the downwelling branch.

The first thing to be confirmed is that subduction does exist in the northern SCS. The ventilated thermocline in the northern SCS has been studied previously. The seasonal variability of the mixed layers and seasonal thermoclines along 115.25° E are depicted here to study the thermocline ventilation in the SCS (Fig. 5). The mixed layer in the northern SCS reaches its maximum in January and it deepens gradually from south to north. The horizontal distribution of mixed layer depth in January is shown in Fig. 6. The mixed layer is deeper in the northwest and shallower in the southeast due to the northwestward Ekman transport as a consequence of the northeast monsoon in January. Besides, the temperature has a strong meridional gradient and part of the water mass with the temperature between 23° and 27° intersects the bottom of the

OSD
11, 1191–1212, 2014

mixed layer (Fig. 5a), this structure is propitious to thermocline ventilation theoretically (Huang, 1990; Wang et al., 2001). Under the action of mechanical and buoyancy forcing the mixed layer seasonally shallows and deepens (Marshall et al., 1993). In spring (Fig. 5b), the sea surface heating is the strongest of the year and the mixed layer depth reaches its minimum. The depth of the mixed layer is very small and the thermocline extends nearly to the sea surface in the northern SCS. The outcrop thermocline is helpful to air–sea heat and momentum exchange and serves as a kind of ventilation thermocline (Liu et al., 2000; Wang et al., 2001). As a result of the shoal of the mixed layer in April, some fluid in the northern SCS (for example the water mass with the temperature between 23° and 27°) leaves the mixed layer, irreversibly subducts into and remains in the thermocline. The subducted water flows southward along the isopycnals in the following months (Fig. 5c and d). So the phenomena of ventilated thermocline and subduction do exist in the northern SCS.

4.2.2 Calculation of the subduction rate

According to Marshall (1993), the annual mean subduction rate S_{ann} is determined as

$$S_{\mathrm{ann}} = -\overline{w}_H - \overline{u}_H \nabla H \tag{2}$$

Here the overbar denotes an annual mean. The effective vertical velocity $\overline{w}_H$ has to be determined from the annual-mean Ekman pumping velocity $\overline{w}_{\mathrm{EK}}$ and a correction term which results from the vorticity balance constraint, $\overline{w}_H = -\overline{w}_{\mathrm{EK}} + \frac{\beta}{f}\int_{-H}^{0}\overline{v}\mathrm{d}z$, f is planetary vorticity and β is its gradient, enabling Eq. (2) to be written as

$$S_{\mathrm{ann}} = -\overline{w}_{\mathrm{EK}} + \frac{\beta}{f}\int_{-H}^{0}\overline{v}\mathrm{d}z - \overline{u}_H \cdot \nabla H \tag{3}$$

The term $\overline{w}_{\mathrm{EK}}$ denotes Ekman pumping, $\overline{u}_H$ denotes the velocity at the mixed layer depth H (defined as the depth at which σ_θ differs by 0.125 from the surface σ_θ). We estimate the annual subduction rate in the SCS according to Eq. (3). It has been pointed

OSD
11, 1191–1212, 2014

out that although detrainment occurs during a substantial period of the seasonal cycle, water subducted into the permanent thermocline is strongly biased toward the winter properties due to the rapid shoaling of the mixed layer in early spring (Stommel, 1979; Marshallet al., 1993; Qiu et al., 1995). So the January mixed-layer depth H from the SODA data is used. The annual-mean $\overline{w}_{EK}$ is calculated from the NCEP monthly climatology data (Fig. 7a) and $\overline{u}_H$ is obtained by interpolating the SODA velocity data to the depth of the mixed-layer in January (Fig. 7b). It should be noted that the estimate of annual subduction rate is subject to substantial error but it can be used to investigate the distribution pattern qualitatively. The distribution of subduction rate is shown in Fig. 7c. The subduction rate calculated should always be nonnegative because it is defined only for the effectively detrained water (Qiu et al., 1995). A negative rate of subduction implies that no effectively detrained water exist. So we change all the negative values into zero. Significant subduction exists in the northern SCS, which amounted to about 1.4 Sv. The magnitude of subduction rate is close to the Ekman pumping rate there, which implies that Ekman pumping takes up a larger portion compared to the lateral induction. This value is also close to the strength of the meridional overturning circulation, so it can be sufficiently concluded that subduction contributes significantly to the downwelling branch of the shallow meridional overturning circulation.

Note that strong subduction also exists between 8° N and 15° N off Vietnam. This is different from the subduction in the northern SCS. The Ekman pumping takes up a larger portion in the northern SCS, so the subduction is an annual mean result. But the Ekman pumping is positive off Vietnam coast (Fig. 7a), which does no contribution to the subduction. The second term on the right side of Eq. (3) is small compared with the lateral induction, so it is the great winter lateral induction at the bottom of mixed layer that leads to strong subduction rate in this zone, which is about 4.4 Sv. However, there is great upwelling off Vietnam in summer, and it can counteract the subduction here on annual mean scale. The upwelling will be discussed in Sect. 4.3.

OSD
11, 1191–1212, 2014

4.3 Upwelling in the southern SCS

Summer upwelling off the Vietnam coast has been pointed out by many studies (Xu et al., 1982; Shaw et al., 1994; Kuo et al., 2000; Xie et al., 2003). Xu et al. (1982) calculated the sea surface dynamic heights in the SCS and showed that there is a relatively low sea surface height region offshore from central Vietnam in summer, indicating occurrence of upwelling in that area. Huang et al. (1994) pointed out that cold water upwelling occurs very often along the western coast of the SCS from Mainland China to the central Vietnamese coast. Kuo et al. (2000) pointed out that the alongshore component of wind stress in summertime caused offshore Ekman transport, which appeared to be the dominant mechanism to pump the cold water upward to the surface along the Vietnamese coast. And high resolution NASA's Quick Scatterometer (QuikSCAT) observations reveal an intense open-ocean pumping associated with the strong offshore increase in southwesterly winds off the Vietnamese coast (Xie et al., 2003). Xie et al. (2003) studied the wind stress distribution in the SCS using a set of satellite data and found a wind jet in summer when the southwesterly winds prevailed. The axis of this wind jet divided the SCS into two parts, with Ekman upwelling and downwelling prevailing in the northern and southern parts respectively (see Xie et al., 2003, their Fig. 2b).

The wind field (Fig. 8) from the NCEP data shows that the wind along the Vietnam coast in July is mostly in the alongshore direction, and this can induce coastal upwelling. Besides, alongshore winds have a significant offshore increase, which causes great positive Ekman pumping in the open ocean off Vietnam. The Ekman pumping rate off Vietnam in July is calculated from the wind stress curl. Assuming for the high estimate that all the Ekman pumping water will be upwelled into the mixed layer and becomes permanently transformed, yields an upwelling transport of 7.3 Sv. However, a large portion of the upwelling is counteracted in annual mean by the winter subduction of about 4.4 Sv off Vietnam (discussed in Sect. 4.2.2).

Discussion Paper | Discussion Paper | Discussion Paper | Discussion Paper |

OSD

11, 1191–1212, 2014

Shallow meridional overturning circulation of the South China Sea

N. Zhang et al.

Title Page
Abstract Introduction
Conclusions References
Tables Figures
◀ ▶
Back Close
Full Screen / Esc
Printer-friendly Version
Interactive Discussion

5 Comparison with the cross-equatorial cell in the Indian Ocean

The shallow meridional overturning circulation in the SCS and the cross-equatorial cell (CEC) in the Indian Ocean have both similarities and differences. In the Indian Ocean, subduction occurs dominantly in the Southern Hemisphere and upwelling in the Northern Hemisphere, in the Somali and Arabian coastal upwelling areas, leading to a cross-equatorial shallow cell (Miyama et al., 2003). The CEC (about 6 Sv, see Fig. 2 in Miyama et al., 2003) is stronger than the meridional overturning circulation in the SCS. The north Indian Ocean is also situated in a monsoon area. Different from the SCS, the summer monsoon winds dominate the annual circle in the Indian Ocean. It is predominantly antisymmetric about the equator with westlies (eastlies) north (south) of the equator. Thus the return flow from northern upwelling to southern subduction occurs by southward cross-equatorial Ekman transport. The subduction rate in the South Indian Ocean is also estimated by Karstensen and Quadfasel (2002) according to Eq. (3). They indicated that a total of 34 Sv is subducted into density classes 23–27 $\mathrm{kg\,m^{-3}}$. Out of these, 9.5 Sv enter into densities $< 25.7\,\mathrm{kg\,m^{-3}}$, corresponding to about 150 m upwelling depth off Somalia. Somali upwelling occurs at the offshore-flowing flanks of the Souther Gyre at 3–5° N and of the Great Whirl. From heat flux considerations, Shott et al. (2002) estimates that only the lighter fraction of the offshore flow could be warmed enough during the course of the monsoon to become surface waters. This yielded a total upwelling rate of 4.2 Sv as an annual mean. There is an approximate balance between the independent estimates of cross-equatorial subsurface northward Somali Current transport, of Somali upwelling and of southward Ekman return flow across the equator. For the shallow meridional overturning circulation in the SCS, the Ekman transport (0.91 Sv) and the subduction rate in the northern SCS (1.4 Sv) are of the same order of magnitude. But the upwelling rate obtained off the Vietnam coast seems not match with them. Two reasons account for this. First, we assume that all the Ekman pumping water will be upwelled into the mixed layer and becomes permanently transformed when estimating the upwelling rate, so this yields

OSD
11, 1191–1212, 2014

a high estimate. Second, a large portion of the upwelling is counteracted in annual mean by the subduction of about 4.4 Sv off Vietnam.

6 Discussion and conclusions

In this paper, we investigate the climatological annual mean shallow meridional overturning circulation in the SCS and explore its formation mechanism. The shallow meridional overturning circulation consists of northward surface flow above 50 m, a downwelling branch in the north at about 19° N, a southward return subsurface flow between 50 m and 400 m and an upwelling branch in the south between 8° N and 12° N.

The annual mean zonal wind stress is westward at most latitudes of the SCS, which drives northward Ekman drift in the surface. The magnitude of Ekman transport at 18° N (0.91 Sv) is close to the strength (1 Sv) of the shallow meridional overturning circulation. This confirms that the surface northward flow is mainly driven by the westward zonal wind component of the annual mean wind stress. Under the influence of mechanical and buoyancy forcing, the mixed layer in the SCS seasonally shallows and deepens intensely. In winter, the depth of mixed layer reaches a maximum, deepening gradually from south to north and the density has a strong meridional gradient. In spring, as a result of the sudden shoaling of the mixed layer depth, the thermocline outcrops in the northern SCS, part of mixed layer water mass subducts into the thermocline and flows southward along the isopycnals. The subduction rate in the northern SCS is estimated to be about 1.4 Sv. The subduction contributes significantly to the downwelling branch. The upwelling region is mainly along the Vietnam coast and in the open-ocean off the coast. Part of the upwelling is induced by alongshore winds along the Vietnam coast in summer. And the alongshore winds have a significant offshore increase, which causes great positive Ekman pumping in the open ocean off Vietnam. Assuming for the high estimate that all this water will be upwelled into the mixed layer and becomes permanently transformed, yields an upwelling transport of 7.3 Sv. However, a large

Discussion Paper | Discussion Paper | Discussion Paper | Discussion Paper |

OSD

11, 1191–1212, 2014

Shallow meridional overturning circulation of the South China Sea

N. Zhang et al.

portion of the upwelling is counteracted in annual mean by the subduction of about 4.4 Sv in winter in this zone.

It is worth noting that this paper discusses the shallow meridional overturning circulation and its dynamics on the annual-mean scale. But there may be different driving mechanisms when discussing them in different seasons. We will discuss this in a further study.

Acknowledgements. This research was supported by the National Basic Research Program of China (2011CB403502), by the National Natural Science Foundation of China (41276011 and 41221063), and by Research Project of Chinese Ministry of Education (113041A). The authors wish to thank the reviewers and editors for their valuable constructive comments.

References

Cabanes, C., Lee, T., and Fu, L.: Mechanisms of interannual variations of the meridional overturning circulation of the north Atlantic Ocean, J. Phys. Oceanogr., 38, 467–480, 2008.

Carton, J. A., Chepurin, G., and Cao, X.: A simple ocean data assimilation analysis of the global upper ocean 1950–1995. Part I: Methodology, J. Phys. Oceanogr., 30, 294–309, 2000.

Huang, Q., Wang, W., Li, Y., and Li, C.: Current characteristics of the South China Sea, Oceanology of China Sea, 1, 39–47, 1994.

Huang, R. X.: On the three-dimensional structure of the wind-driven circulation in the North Atlantic, Dynam. Atmos. Oceans, 15, 117–159, 1990.

Iselin, C. O. D.: The influence of vertical and lateral turbulence on the characteristics of the waters at mid-depths, Trans. Amer. Geophys. Union, 20, 414–417, 1939.

Kuo, N., Zheng, Q., and Ho, C. R.: Satellite observation of upwelling along the western coast of the South China Sea, Remote Sens. Environ., 74, 463–470, 2000.

Liu, C., Du, Y., Zhang, Q., and Wang, D.: Seasonal variation of subsurface and intermediate water masses in the South China Sea, Oceanologia et Limnologia Sinica 39, 55–64, 2008 (in Chinese with English abstract).

Liu, Q., Yang, H., annd Wang, Q.: Dynamic characteristics of seasonal thermocline in the deep sea region of the South China Sea, Chin. J. Oceanol. Limn., 18, 104–109, 2000.

OSD

11, 1191–1212, 2014

Marshall, J. C., Williams, R. G., and Nurser, A. J. G.: Inferring the subduction rate and period over the North Atlantic, J. Phys. Oceanogr., 23, 1315–1329, 1993.

Masumoto, Y., Sasaki, H., Kagimoto, T., Komori, N., Ishida, A., Sasai, Y., Miyama, T., Motoi, T., Mitsudera, H., Takahashi, K., Sakuma, H., and Yamagata, T.: A fifty-year eddy-resolving simulation of the world ocean: preliminary outcomes of OFES (OGCM for the earth simulator), J. Earth Simulator, 1, 35–56, 2004.

Miyama, T., McCreary, J. P., Jensen, T. G., Loschnigg, J., Godfrey, S., and Ishida, A.: Structure and dynamics of the Indian-Ocean cross-equatorial cell, Deep-Sea Res. Pt. II, 50, 2023–2047, 2003.

Qiu, B. and Huang, R.: Ventilation of the North Atlantic and North Pacific: subduction versus obduction, J. Phys. Oceanogr., 25, 2374–2390, 1995.

Qu, T., Mitsudera, H., and Yamagata, T.: Intrusion of the North Pacific waters into the South China Sea, J. Geophys. Res., 105, 6415–6424, 2000.

Sasaki, H., Sasai, Y., Kawahara, S., Furuichi, M., Araki, F., Ishida, A., Yamanaka, Y., Masumoto, Y., and Sakuma, H.: A series of eddy-resolving ocean simulations in the world ocean: OFES (OGCM for the Earth Simulator) project, in: Ocean'04, MTTS/IEEE Techno-Ocean'04, vol. 3, Inst. of Electr. and Electron. Eng., New York, 1535–1541, 2004.

Schott, F. A., Dengler, M., and Schoenefeldt, R.: The shallow overturning circulation of the Indian Ocean, Prog. Oceanogr., 53, 57–103, 2002.

Shaw, P. and Chao, S.: Surface circulation in the South China Sea, Deep-Sea Res. Pt. I, 41, 1663–1683, 1994.

Song, Wei, Lan, Jian, Liu, Qinyan, Sui, Dandan, Zeng, Lili, and Wang, Dongxiao: Decadal variability of heat content in the South China Sea inferred from observation data and an ocean data assimilation product, Ocean Sci., 10, 135–139, doi:10.5194/os-10-135-2014, 2014.

Stommel, H.: Determination of water mass properties of water pumped down from the Ekman layer to the geostrophic flow below, P. Natl. Acad. Sci. USA, 76, 3051–3055, 1979.

Su, J.: Overview of the South China Sea circulation and its dynamics, Acta Oceanologica Sinica, 27, 1–8, 2005 (in Chinese with English abstract).

Wang, D., Du, Y., and Shi, P.: Evidence for thermocline ventilation in the South China Sea in winter, Chinese Sci. Bull., 46, 758–762, 2001.

Wang, D., Liu, X., Wang, W., Du, Y., and Zhou, W.: Simulation of meridional overturning in the upper layer of the South China Sea with an idealized bottom topography, Chinese Sci. Bull., 49, 740–747, 2004.

OSD
11, 1191–1212, 2014

Shallow meridional overturning circulation of the South China Sea

N. Zhang et al.

Wang, D., Liu, Q., Huang, R., Du, Y., and Qu, T.: Interannual variability of the South China Sea throughflow inferred from wind data and ocean data assimilation product, Geophys. Res. Lett., 33, L14605, doi:10.1029/2006GL026316, 2006.

Woods, J. D.: The physics of pycnocline ventilation, in: Coupled Ocean–Atmosphere Models, edited by: Nihoul, J. C. J., Elsvier Sci. Pub., 543–590, 1985.

Xie, S., Xie, Q., and Wang, D.: Summer upwelling in the South China Sea and its role in regional climate variations, J. Geophys. Res., 108, 1–13, 2003.

Xu, X. Z., Zhang, Q. Z., and Chen, H.: The general descriptions of the horizontal circulation in the South China Sea, in: Proc. Symp. Chin. Soc. Mar. Hydrol. Meterol., Science Press, Beijing, 119–127, 1982.

Yang, H. and Wu, L.: Trends of upper-layer circulation in the South China Sea during 1959–2008, J. Geophys. Res., 117, C08037, doi:10.1029/2012JC008068, 2012.

OSD
11, 1191–1212, 2014

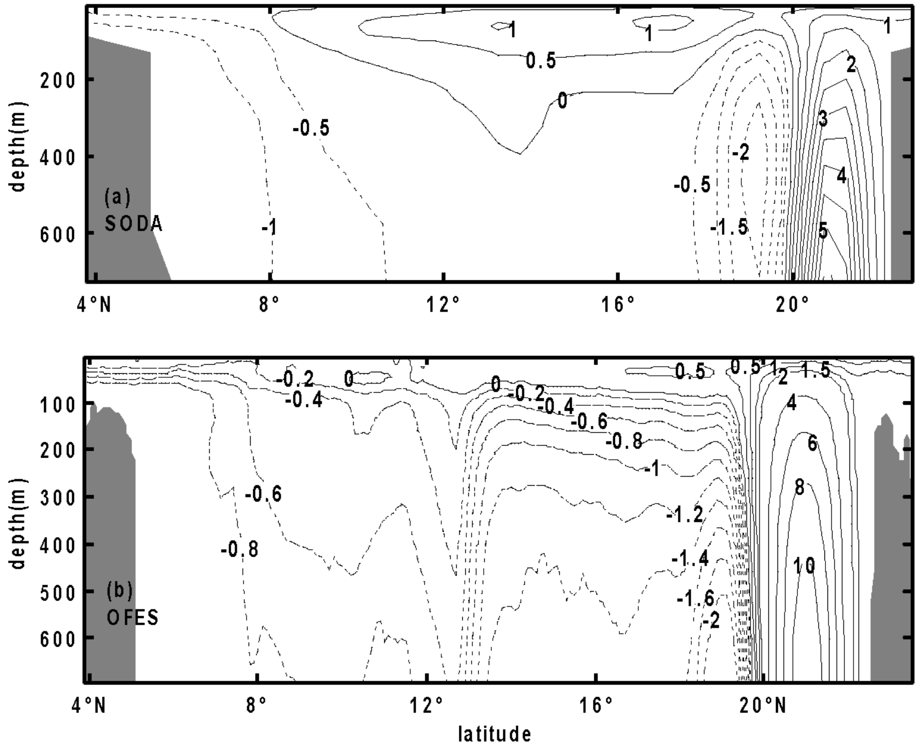

Fig. 1. Annual-mean meridional overturning circulation in the SCS (unit: Sv, 1 Sv = $10^6\ m^3\ s^{-1}$). **(a)** is calculated from SODA data; **(b)** is from OFES data.

OSD
11, 1191–1212, 2014

Shallow meridional overturning circulation of the South China Sea

N. Zhang et al.

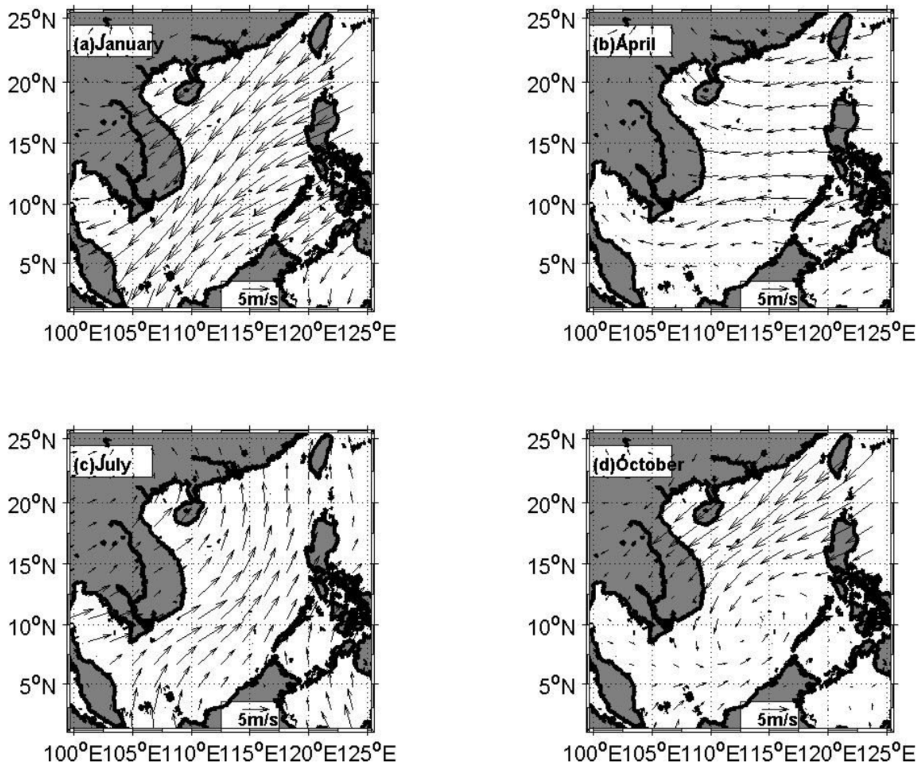

Fig. 2. Monsoon wind fields from the NCEP monthly climatology for **(a)** January, **(b)** April, **(c)** July and **(d)** October.

OSD
11, 1191–1212, 2014

Shallow meridional overturning circulation of the South China Sea

N. Zhang et al.

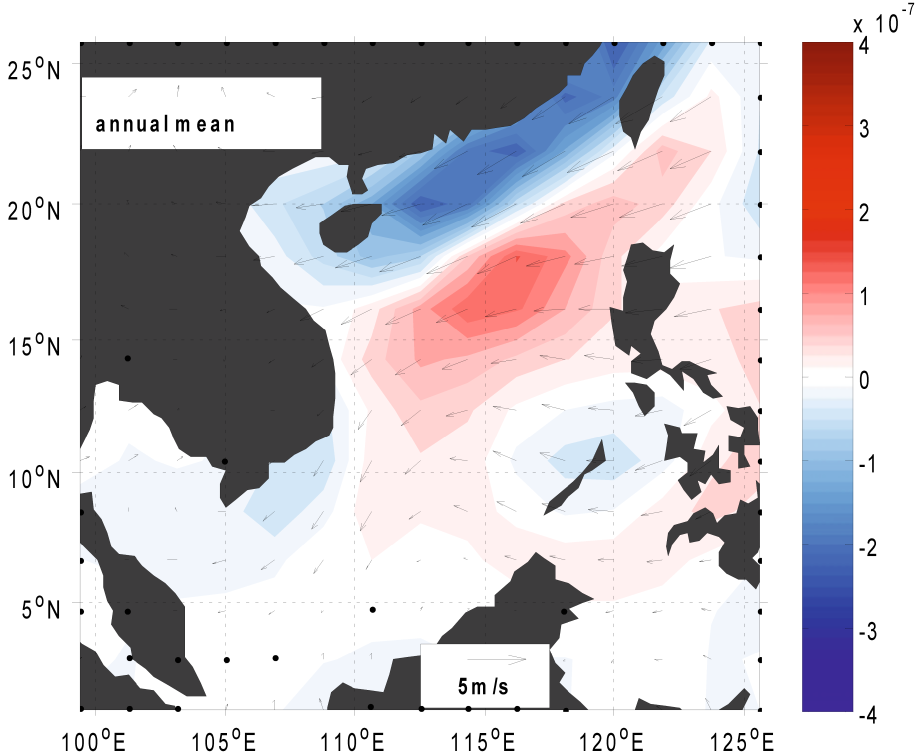

Fig. 3. Annual-mean wind stress (arrows) and wind-curl (contours) for the SCS. The contour interval for wind curl is $0.2 \times 10^{-7}\,\mathrm{N\,m^{-3}}$.

OSD
11, 1191–1212, 2014

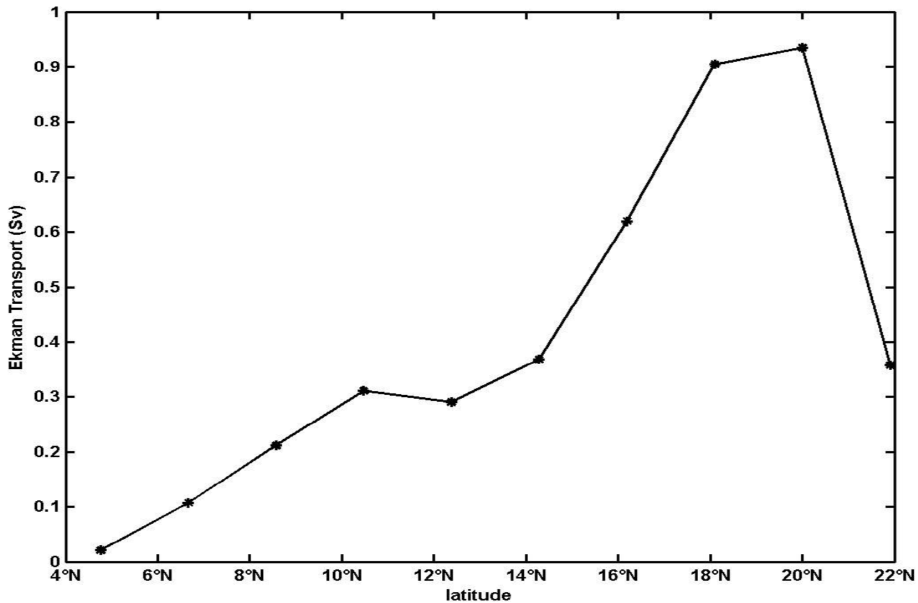

Fig. 4. Annual-mean meridional Ekman transport in the SCS calculated from $\frac{-\tau^x(0)}{f\rho}$.

OSD
11, 1191–1212, 2014

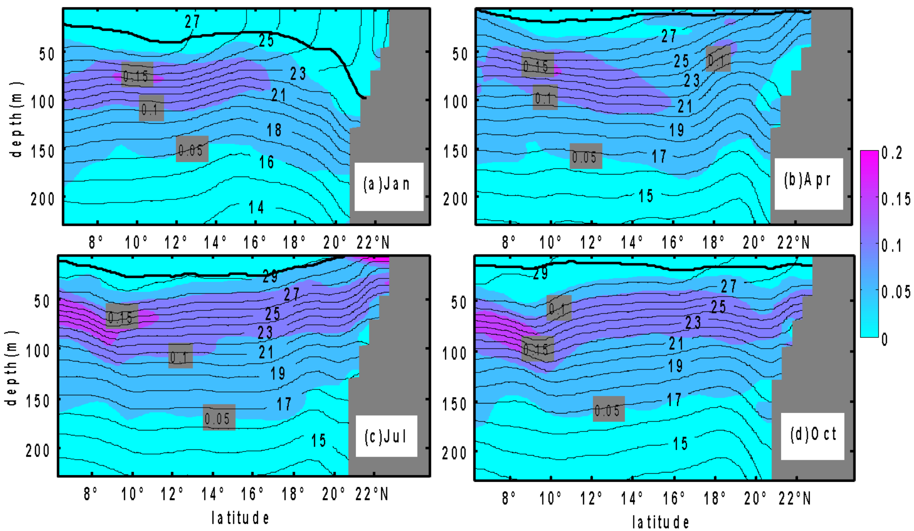

Fig. 5. Temperature (contours) and mixed layer depth (the thick solid line) at 115.25° E section from SODA in different seasons; underlaid are vertical temperature gradients (the units are $^{\circ}\mathrm{C\,m^{-1}}$).

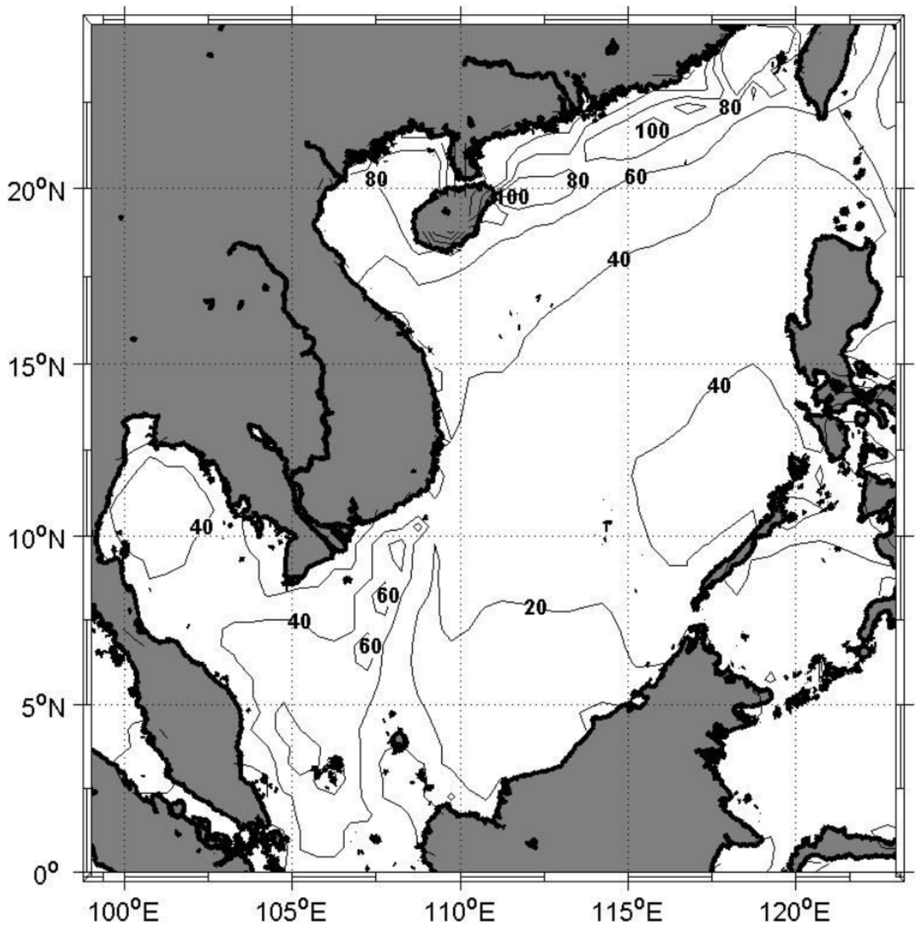

Fig. 6. The horizontal distribution of mixed layer depth in January (unit: m).

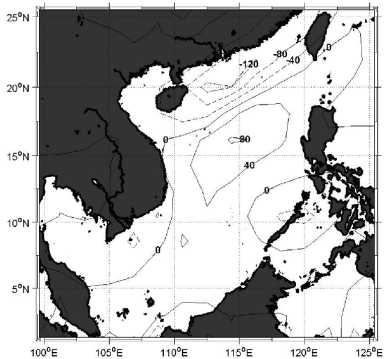

(a) $\overline{w}_{Ek}$ (unit:m/yr)

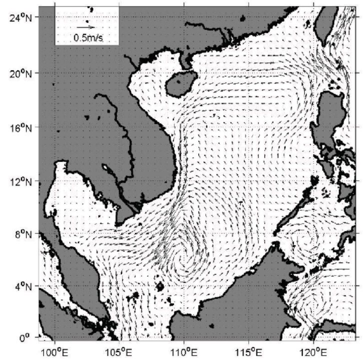

(b) The velocity field at the bottom of the mixed layer in January

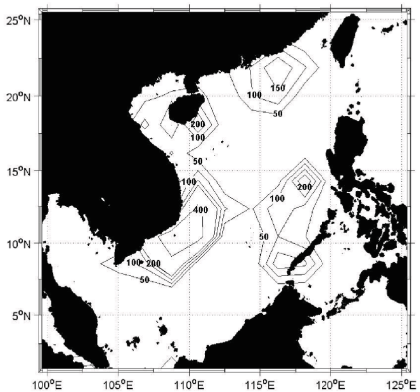

(c) Annual subduction rate in the SCS (unit:m/yr)

Fig. 7. (a) $\overline{w}_{\mathrm{Ek}}$ (unit: $\mathrm{m\,yr^{-1}}$); **(b)** the velocity field at the bottom of the mixed layer in January; **(c)** annual subduction rate in the SCS (unit: $\mathrm{m\,yr^{-1}}$).

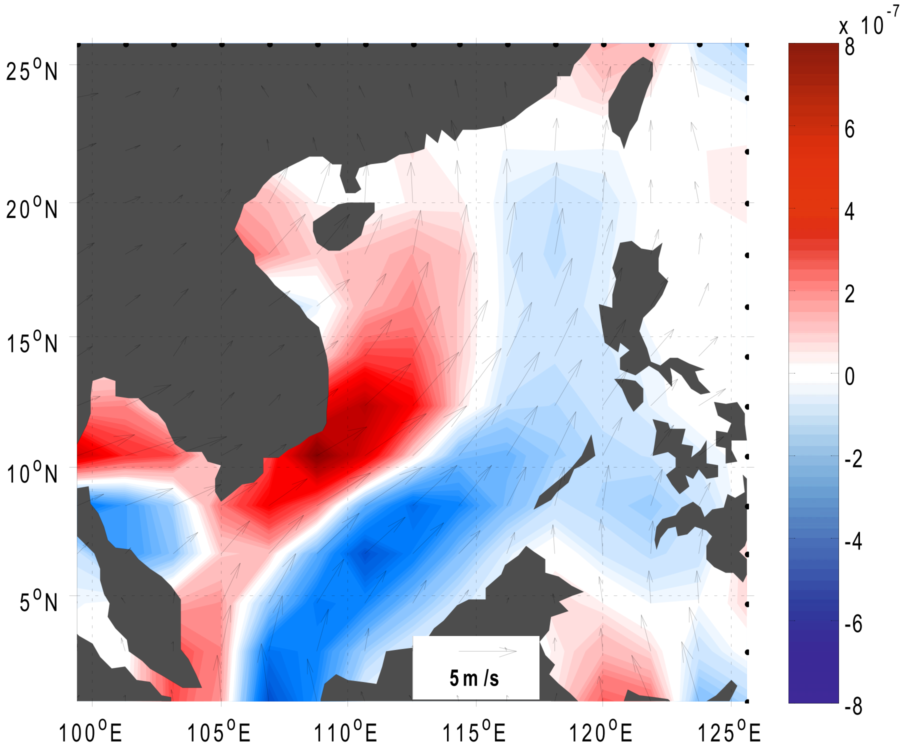

Fig. 8. Same as in Fig. 3, but for July.

OSD
11, 1191–1212, 2014
Shallow meridional overturning circulation of the South China Sea
N. Zhang et al.